



OPEN

## Safety evaluation of extracellular vesicles derived from hypoxia primed mesenchymal stem cells of umbilical cord and adipose tissue

Quyen Thi Nguyen<sup>1,6</sup>, Nhung Thi Hong Dinh<sup>1,6</sup>, Ngo Thu Hang<sup>2</sup>, Can Van Mao<sup>2</sup>, Xuan-Hai Do<sup>3</sup>, Duc Son Le<sup>1</sup>, Hong-Nhung Dao<sup>1</sup>, T. Ngan Giang<sup>1</sup>, Nicholas Forsyth<sup>4</sup>, Van T. Hoang<sup>1</sup>✉ & Liem Nguyen Thanh<sup>1,5</sup>✉

Extracellular vesicles (EVs) hold great promise as regenerative therapeutics due to their roles in intercellular communication and tissue repair. This study aimed to assess the safety of EVs derived from human mesenchymal stem cells (MSCs) obtained from both umbilical cord (UC-MSC-EVs) and adipose tissue (AD-MSC-EVs) sources, which were manufactured under xeno- and serum-free conditions and primed with 5% O<sub>2</sub>. EVs from neither source caused vascular or muscular stimulation in New Zealand rabbits. Systemic hypersensitivity tests revealed that neither UC-MSC-EVs nor AD-MSC-EVs triggered significant changes in allergic and immune responses or hematological parameters in the animals, highlighting their biocompatibility and safety when administered systemically. Furthermore, acute toxicity test using Swiss mice showed all mice survived without any signs of acute toxicity after intravenous injection of both types of EVs at very high doses (up to 10,000 µg/kg of body weight). In addition, subchronic toxicity examination in Wistar rats revealed that repeated injections of neither UC-MSC-EVs nor AD-MSC-EVs (50–150 µg/animal) affected hematological indices or the functions of the liver, kidney, or spleen. Collectively, our findings provide strong evidence that both UC-MSC-EVs and AD-MSC-EVs manufactured under xeno- and serum-free conditions and primed with 5% O<sub>2</sub> are safe for potential therapeutic use. These results contribute to the growing body of evidence supporting the safety of physoxic MSC-derived EVs as therapeutic drugs, confirming their potential for applications in regenerative medicine.

**Keywords** Mesenchymal stem cells, Extracellular vesicle, Safety, Vascular and muscular stimulation, Systemic hypersensitivity, Acute toxicity, Subchronic toxicity

### Abbreviations

EVs	Extracellular vesicles
MSCs	Mesenchymal stem cells
MSC-EVs	MSCs-derived EVs
AD-MSC-EVs	MSC-EVs from adipose tissue
UC-MSC-EVs	MSC-EVs from both umbilical cord
NTA	Nanoparticle tracking analysis
TEM	Transmission electron microscopy
PDT	Population doubling time
P	Passages
BCA	Bicinchoninic acid
HE	Hematoxylin and eosin

<sup>1</sup>Vinmec Research Institute of Stem Cell and Gene Technology, College of Health Sciences, Vin University, Vinhomes Ocean Park, Gia Lam District, Hanoi 12400, Vietnam. <sup>2</sup>Department of Pathophysiology, Vietnam Military Medical University, 160 Phung Hung, Ha Dong, Hanoi, Vietnam. <sup>3</sup>Department of Practical and Experimental Surgery, Vietnam Military Medical University, 160 Phung Hung, Ha Dong, Hanoi, Vietnam. <sup>4</sup>University of Aberdeen, King's College, Aberdeen AB24 3FX, UK. <sup>5</sup>Department of Regenerative Medicine and Cell Therapy, Vinmec Times City International Hospital, Vinmec Healthcare System, 458 Minh Khai, Hanoi 11622, Vietnam. <sup>6</sup>Quyen Thi Nguyen and Nhung Thi Hong Dinh contributed equally to this work. ✉email: van.ht@vinuni.edu.vn; liem.nt@vinuni.edu.vn

RBCs	Red blood cells
WBCs	White blood cells
IL	Interleukin
TNF	Tumor necrosis factor
ELISA	Enzyme-linked immunosorbent assay
LD <sub>50</sub>	Median lethal dose
AST	Aspartate aminotransferase
ALT	Alanine aminotransferase
SEMs	Standard errors of the means

Extracellular vesicles (EVs) are lipid bilayer structures that are secreted by cells into the extracellular space ranging in size from 30 to 5000 nm<sup>1,2</sup>. These nanosized structures are recognized as essential messengers that play pivotal roles in intercellular communication<sup>1,3</sup>. EVs carry bioactive molecules such as proteins, lipids, nucleic acids, and metabolites and are capable of transporting these cargos to other cells, often at distant locations, influencing various cellular processes<sup>4,5</sup>.

Mesenchymal stem cells (MSCs) are stromal cells that can be isolated from various tissues, with the most common sources including bone marrow, adipose tissue, and the umbilical cord<sup>6</sup>. MSCs are characterized by their multipotent differentiation potential enabling them to give rise to a variety of cell types, such as those representative of bone, cartilage, fat, and muscle cells<sup>7</sup>. In addition, MSC can modulate the immune response, reducing inflammation and promoting tissue healing through their immunomodulatory effects<sup>8</sup>. These unique qualities make MSCs a valuable resource for tissue regeneration and repair, and they have become a subject of extensive research and clinical interest. Although MSC therapy offers promising therapeutic benefits, there are several challenges that must be addressed before it can be widely adopted for clinical use. These challenges include concerns about cell rejection, the undesired differentiation of MSCs, the accumulation of MSCs in unintended locations, and the risk of tumorigenesis<sup>9</sup>. Therefore, cell-free therapeutic tools with similar regenerative properties might be attractive alternatives for the treatment of diseases.

Various data obtained in experimental animals have shown that MSC-derived EVs (MSC-EVs) and MSCs have comparable therapeutic effects in terms of immunomodulation, tissue regeneration, and angiogenesis<sup>10</sup>. In addition, MSC-EVs overcome many of the challenges of MSC-based therapy, as they lack immunogenicity<sup>11</sup>, do not undergo unplanned differentiation<sup>12</sup>, and presenting the opportunity for production and use as an off-the-shelf drug in a lyophilized form<sup>9,13–15</sup>. For these reasons, there is an urgent need to explore the potential of MSC-EVs in experimental and clinical settings.

Although MSC-EVs are valuable biological agents, the scale-up of their manufacturing for clinical use remains challenging, as they are present in limited numbers under normal MSC culture conditions. Hypoxia, or physoxia preconditioning can optimize the performance of MSCs better reflecting the physiological conditions of the cells within many tissues in the body<sup>16–19</sup>. MSCs cultured under physoxia have been shown to release more EVs, which have a distinct protein profile<sup>20,21</sup> and are enriched in survival and angiogenic factors<sup>22</sup>. However, while these studies have focused on the *in vitro* biological properties of EVs under physoxic conditions, *in vivo* evaluations of physoxic EVs in animals remain lacking. Further, EVs from MSC cultures in medium containing serum or/and animal-derived components are unsuitable for clinical applications due to their unknown and undefined compositions<sup>23,24</sup>. Therefore, it is crucial to elucidate MSC-EVs changes in reaction to physoxia and xeno-free and serum-free culture conditions and their *in vivo* behaviors.

To address this research gap, this study aimed to evaluate the impact of physoxia and xeno- and serum-free conditions on the biological properties of EVs isolated from umbilical cord- and adipose tissue-derived MSCs (UC-MSC-EVs and AD-MSC-EVs, respectively) *in vitro* and assess their safety profiles (local stimulation, systemic hypersensitivity, acute toxicity, and subchronic toxicity) *in vivo* using animals (New Zealand white rabbits, Swiss mice, and Wistar white rats) (Fig. 1). The outcomes of this study are expected to provide an important insight into the potential of physoxic MSC-EVs for clinical translation in therapeutic applications.

## Methods

### Animals

The work has been reported in line with the ARRIVE guidelines 2.0. Animals, including New Zealand white rabbits (1.8–2.3 kg, 4–4.5 months old), Wistar rats (200–300 g, 12–14 weeks old), and Swiss mice (20–30 g, 6–8 weeks old), were obtained from Le Thi Mo's business household and housed in separate cages in a climate controlled environment room with a 12-hour light/dark cycle and no restriction food and water (Vietnam Military Medical University). Animal handling and the experimental procedures were reviewed and approved by the Institutional Review Board (IRB) of Dinh Tien Hoang Institute of Medicine and were performed according to the Guidelines for Animal Experiments of the IRB (No. IRB-A-2201). Before sacrifice, animals were anesthetized using isoflurane (Baxter, USA). Animals were initially anesthetized with 5% isoflurane in oxygen at a flow rate of 1 L/min to induce loss of consciousness. While fully anesthetized, an intraperitoneal injection of pentobarbital sodium (100 mg/kg) was administered to induce irreversible cessation of vital functions. Death was confirmed by the absence of heartbeat and respiration prior to proceeding with subsequent experimental procedures.

### MSC isolation and culture

Umbilical cord and adipose tissue samples were obtained from women after obtaining consent forms from the participants and approval from the Ethics Council of Vinmec International Hospital (No.03/2022/QĐ-VNC). Birth was by cesarean section, and samples were immediately placed in 0.9% sodium chloride (Bidiphar, Vietnam). MSCs were isolated using enzymatic digestion as described previously<sup>26</sup>. Briefly, the tissues were cut into small fragments and incubated in 500 U/ml collagenase type I (Sigma, Germany) for 150 min, 37 °C,

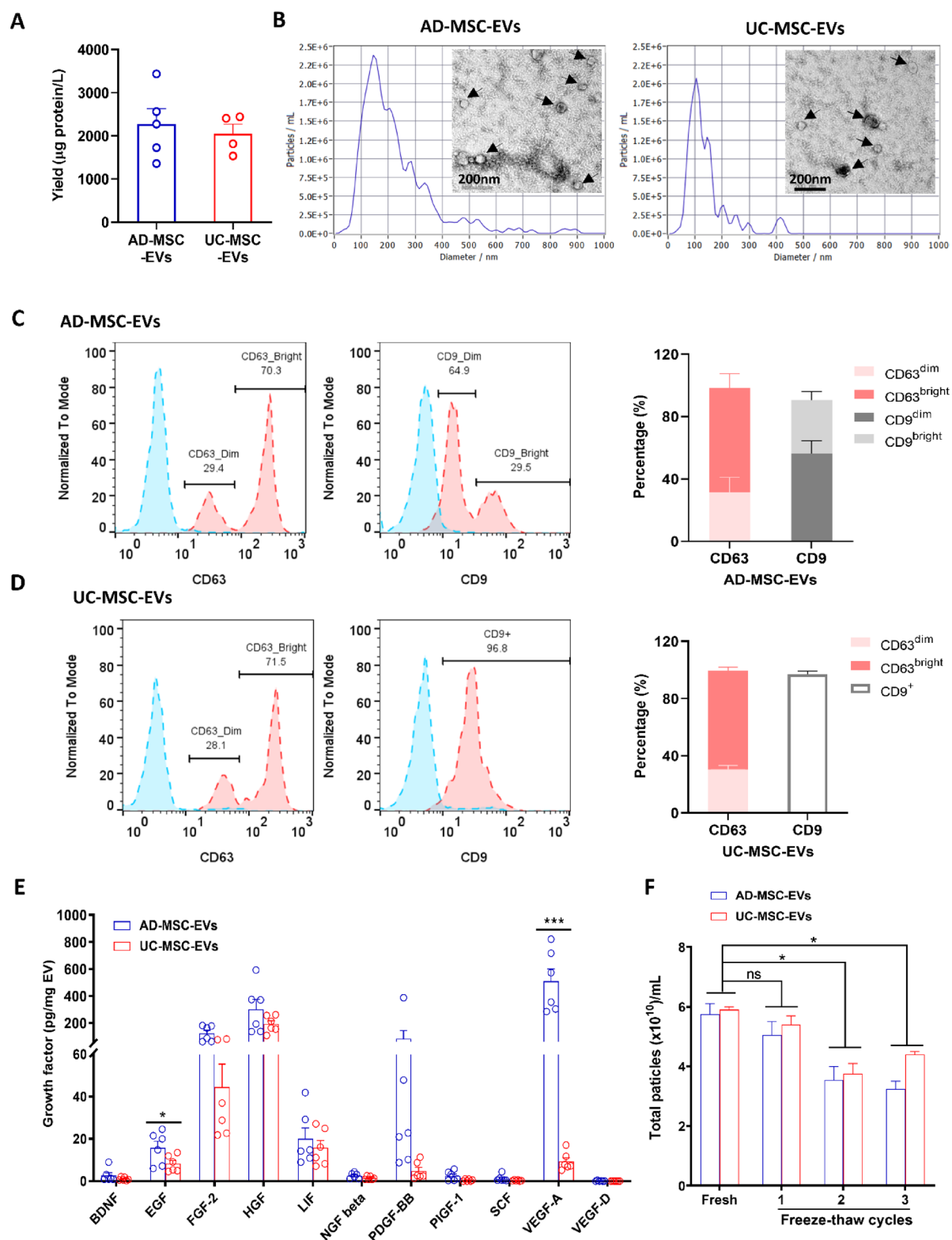


**Fig. 1.** MSC-EV characterization. (A) Yield of EVs (total amount of EVs per liter of culture medium, mg/L). (B) TEM image of the isolated EVs. (C, D) Flow cytometry analysis of MSC-EV surface markers, including CD63 and CD9. “Dim” and “bright” CD9/CD63 populations were gated based on fluorescence intensity with “dim” indicating low and “bright” indicating high marker expression. (E) Analysis of the profiles of growth factors released from AD-MSC-EVs and UC-MSC-EVs by Luminex assay. (F) Stability of EVs after multiple freeze-thaw cycles. The data are presented as mean  $\pm$  SEM. Significant differences between groups in Figure E and F were analyzed by t-test and ANOVA/Bonferroni, respectively.

300 rpm using an GentleMACS Dissociator. The isolated cells were counted by Trypan blue staining and were then plated at 3,200 cells/cm<sup>2</sup> in culture flasks coated with CTS™ CELLstart™ substrate (Gibco, USA). Primary cells were cultured in StemMACS™ MSC Expansion Medium (Miltenyi Biotec, Germany) at 37 °C with 5% CO<sub>2</sub> under ambient oxygen (21% oxygen). MSCs were harvested when the cells reached 80% confluence. For long-term storage, MSCs were cryopreserved at passages (P) 1 and 3 in serum-free, xeno-free medium containing defined reagents (CryoStorR CS10 (Stemcell Technologies, Singapore)) in the vapor phase of liquid nitrogen. The temperature of the cells was monitored and maintained at -196 °C.

For subsequent analysis, a cryopreserved stock of AD-MSCs and UC-MSCs at P3 was thawed and cultured in StemMACS™ MSC Expansion Medium (Miltenyi Biotec, Germany) at 37 °C with 5% CO<sub>2</sub> and 21% O<sub>2</sub>. Cells were harvested using TrypLE Select CTS enzyme (Gibco, USA) and passaged at a concentration of 3,200 cells/cm<sup>2</sup>. At the last passage, the cells were grown under 21% O<sub>2</sub> conditions for 3 days, followed by a switch to physoxic conditions of 5% O<sub>2</sub> for 2 days.

### MSC characterization

The population doubling time (PDT) was calculated as described previously<sup>25</sup>. Briefly, MSCs were seeded at a concentration of 5000 cells/cm<sup>2</sup> in triplicate using CTS™ CELLstart™ substrate-coated flasks (Thermo Fisher Scientific, USA) until the culture reached 80% confluence. The cells were harvested, stained with Trypan blue and dye-excluding cells counted using a Neubauer improved C-chip disposable hemacytometer (INCYTO, Germany). The PDT was calculated based on the numbers of cells seeded and harvested.

To further assess cell viability, the harvested cells were stained with DAPI. To analyze MSC identity, the harvested cells were immunolabelled stained with CD90 FITC, CD105 PerCP-Cy5.5, CD73 APC and a negative marker cocktail (CD45/CD34/CD11b/CD19/HLA-DR PE) using a BD Stemflow™ Human MSC Analysis Kit (Beckman Dickson, USA) according to the manufacturer's instructions. The stained cells were acquired with a MACSQuant® Analyzer 10 flow cytometer and analyzed using FlowJo software.

### EV isolation

To isolate EVs, a cryopreserved stock of AD-MSCs and UC-MSCs at P3 were cultured independently in T225 culture flasks under air oxygen (21%) until P5. The cells were then subcultured in HYPERFlasks under air 21% oxygen for 3 days and then switched to 5% oxygen for 2 days. The conditioned medium was then harvested and filtered through a microfiltration membrane (Prefilter PreFlow™ UB) with a pore size of 0.45 µm to remove dead cells and cell debris. Subsequently, the post- microfiltration media was concentrated using a tangential filtration system (Minimate TFF capsule OMEGA) with a 100 kDa hollow-fiber membrane. The concentrated medium was then subjected to ultracentrifugation at 100,000 × g for 75 min at 4 °C. The pellet was finally resuspended in PBS and stored at -80 °C for further experiments. For injection, both UC-MSC-EVs and AD-MSC- EVs were thawed at 4 °C and diluted in Ringer Lactate to the appropriate protein concentration for each test. Final injection volumes were 1 mL (rabbit vascular/muscular stimulation and hypersensitivity tests), 0.2 mL (mouse acute toxicity), and 0.5 mL (rat subchronic toxicity). The injections were performed using sterile syringes and needles. Prior to administration, the injection site was cleaned with 70% ethanol.

### EV characterization

Total protein quantification was carried out using a Pierce BCA Protein Assay Kit (Thermo Scientific™, USA) according to the manufacturer's instructions. Briefly, a standard curve was generated by diluting BSA to concentrations ranging from 20 to 1,000 µg/mL. Subsequently, 10–20 µL of MSC-EVs were mixed with 80–160 µL of the BCA working reagent and incubated for 30 min at 37 °C. The protein content was then measured at 562 nm using a plate reader.

EV morphology was evaluated by transmission electron microscopy (TEM). Briefly, EV samples were prepared at a concentration of at least 1 mg/mL in PBS. The samples were then positioned on copper grids with a 400-mesh size (Electron Microscopy Services, USA). These grids were rinsed with deionized water and subjected to negative staining using a 2% solution of uranyl acetate (Ted Pella, USA). TEM images were captured using a JEM1011 electron microscope (JEOL Ltd., Japan) operating at an accelerating voltage of 100 kV.

Sterility of EV products were confirmed by microbiological and mycoplasma testing. Bacterial and fungal testing was conducted using the BacT/Alert three-dimensional microbial detection system (Biomérieux, USA). Mycoplasma testing was performed using a MycoAlert PLUS *Mycoplasma* detection kit (Lonza, Switzerland), and the results were measured using a Lucetta luminometer (Lonza, Switzerland) following the manufacturer's instructions.

To determine the size distribution of the AD- and UC-MSC-derived EVs by nanoparticle tracking analysis (NTA), the EVs were resuspended in PBS, and 500 µL of the resuspension was loaded into the sample chamber of ZetaView software using a 1 mL syringe. Images of the particles were captured using a ZetaView PMX-230-S device (Particle Metrix, Meerbusch, Germany) with the following settings: 488 nm laser; sensitivity, 80; and shutter, 100. A size distribution histogram was generated using ZetaView PMX software.

For the analysis of exosome biomarkers, at least 2.5 × 10<sup>9</sup> particles were incubated with a mixture of magnetic beads coated with CD9 or CD63 at a 1:1:1 ratio (Abcam, UK) to capture EVs. EVs were then stained with human anti-CD9 FITC and anti-CD63 PE REAfinity™ antibodies (Miltenyi Biotec, Germany) and analyzed using a MACSQuant® Analyzer 10 flow cytometer (Miltenyi Biotec, Germany) and FlowJo software (Beckman Dickson, USA).

To quantify the concentrations of growth factors, Growth Factor 11-Plex Human ProcartaPlex™ Panel kits (Thermo Fisher Scientific, USA) were used following the manufacturer's instructions. Briefly, the EV samples were lysed using RIPA buffer (Thermo Scientific™, USA) prior to the assay and incubated with beads targeting 11 different growth factors: brain-derived neurotrophic factor (BDNF), epidermal growth factor (EGF), fibroblast



growth factor 2 (FGF-2), hepatocyte growth factor (HGF), leukemia inhibitory factor (LIF), nerve growth factor beta (NGF-b), platelet-derived growth factor BB (PDGF-BB), placental growth factor 1 (PlGF-1), stem cell factor (SCF), vascular endothelial growth factor-A (VEGF-A), and VEGF-D. The beads were incubated with a biotin detection antibody followed by staining with a streptavidin-RPE antibody and measured with a Luminex™ Instrument (Thermo Fisher Scientific, USA).

To evaluate the stability of extracellular vesicles (EVs), the particle concentrations of freshly prepared EV samples and after each of three freeze-thaw cycles (with a one-day interval between each cycle) were measured by using a ZetaView PMX. EV integrity after 6 months of storage at  $-80^{\circ}\text{C}$  was also assessed by evaluating particle concentration, size distribution, protein content, and expression of surface markers CD9 and CD63.

To minimize batch-to-batch variation, all EV batches used in the experiments were required to meet the following acceptance criteria: (1) protein concentration of  $15\text{ mg/mL} \pm 20\%$ , (2) expression of EV markers CD9 and CD63 confirmed by flow cytometry, (3) negative results for bacterial, fungal, and mycoplasma contamination, and (4) endotoxin levels below  $0.5\text{ EU/mL}$ .

### In vivo vascular and muscle stimulation tests

New Zealand white rabbits (1.8–2.3 kg, 4–4.5 month old, total 21 animals) were randomly distributed into 3 groups ( $n=7$ ). The rabbits were subjected to vascular stimulation test, which refers to the local response of blood vessels at the injection site and muscle stimulation refers to tissue reactivity following intramuscular injection. For the vascular stimulation test, the rabbits were intravenously injected with  $50\text{ }\mu\text{g}$  of AD-MSC-EVs,  $50\text{ }\mu\text{g}$  of UC-MSC-EVs, or Ringer Lactate as a control via the marginal ear vein. For the muscle stimulation test, the rabbits were intramuscularly injected with the same amount of Ringer Lactate, AD-MSC-EVs, or UC-MSC-EVs via the right quadriceps muscle. The temperature at the site of injection was measured daily. Four days after the treatment, the rabbits were sacrificed. The injection sites were collected and fixed in 4% paraformaldehyde, embedded in paraffin and cut into serial  $5\text{-}\mu\text{m}$  sections, which were then subjected to hematoxylin and eosin (HE) staining. The degree of vascular stimulation and muscle stimulation was assessed via macroscopic observation and histopathological examination. A positive response was defined as  $\geq 1.5^{\circ}\text{C}$  temperature increase or evidence of local inflammation. Images were captured using a microscope (Olympus, Japan).

### In vivo systemic hypersensitivity test

New Zealand white rabbits (1.8–2.3 kg, 4–4.5 month old, total 48 animals) were randomly distributed into 8 groups ( $n=6$ ). The rabbits were repeatedly injected with UC-MSC-EVs and AD-MSC-EVs via the marginal ear vein at a low ( $12.5\text{ }\mu\text{g/animal}$ ), medium ( $50\text{ }\mu\text{g/animal}$ ), or high ( $250\text{ }\mu\text{g/animal}$ ) dose on days 0, 2, and 4. On day 14, a double dose was injected into the respective groups. Rabbits injected with Ringer Lactate and untreated rabbits were used as controls. The body weight and temperature of the rabbits were monitored for 14 days after the first injection. Blood was collected 30 min before each injection and 30 min after the 4th injection. Hematological parameters, including the number of red blood cells (RBCs) and white blood cells (WBCs) and platelet and hemoglobin levels, were investigated. Cytokines related to allergies, such as histamine and IgE, and systemic proinflammatory cytokines, such as interleukin (IL)-6, IL-1 $\beta$ , and tumor necrosis factor (TNF)- $\alpha$ , in the plasma were measured by Enzyme-linked Immunosorbent assay (ELISA) according to the manufacturer's instructions.

### In vivo acute toxicity test

Swiss mice (20–30 g, 8–10 week old, total 54 animals) were randomly distributed into 9 groups ( $n=6$ ). The mice were intravenously injected with different doses (500, 2,000, 5,000, or  $10,000\text{ }\mu\text{g/kg}$  of body weight) of UC-MSC-EVs or AD-MSC-EVs or with Ringer Lactate via the tail vein. The survival rate and body weight of the mice were monitored daily for 14 days to determine the median lethal dose ( $\text{LD}_{50}$ ).

### Subchronic toxicity test

Wistar white rats (200–300 g, 8–10 week old, total 36 animals) were randomly distributed into 6 groups ( $n=6$ ). The rats were intravenously injected with UC-MSC-EVs or AD-MSC-EVs, with either  $50\text{ }\mu\text{g/animal}$  (low dose) or  $150\text{ }\mu\text{g/animal}$  (high dose), three times at 10-day intervals via the tail vein. A group of rats injected with Ringer Lactate and another group that did not receive injections were used as controls. Exercise status, the amount of food consumed, convulsions, diarrhea, and death were monitored throughout the experiment. Blood cell counts were conducted before injection and on day 10 after each injection to determine the WBC, RBC, and platelet counts and hemoglobin levels. Liver and kidney damage was examined by measuring the serum concentrations of aspartate aminotransferase (AST), alanine aminotransferase (ALT), urea, and creatinine before injection and on day 10 after each injection. Histology of the liver, kidney, and spleen was examined using HE staining on day 10 after the final injection.

### Statistical analysis

The data are presented as the means  $\pm$  standard errors of the means (SEMs). Significant differences between two groups were assessed using two-tailed Student's  $t$  tests, and differences among multiple groups were assessed using two-way ANOVA followed by Bonferroni correction (ANOVA/Bonferroni).  $P$  values  $< 0.05$  were considered to indicate statistical significance. All analyses were performed using GraphPad PRISM software (GraphPad).

## Results

### MSC characterization

To characterize AD-MSCs and UC-MSCs exposed to hypoxic conditions (5% oxygen), the morphology of the cells was first examined. Under microscopy, both AD-MSCs and UC-MSCs adhered to the vessel surfaces and

exhibited a spindle-shaped or elongated fibroblast-like shape (Fig. S1A). The PDTs of AD-MSCs and UC-MSCs were  $40.3 \pm 4.6$  h and  $35.0 \pm 4.4$  h, respectively. There was no significant difference in PDT between AD-MSCs and UC-MSCs (Fig. S1B). The viability of the cells was also confirmed; the viability of the AD-MSCs was  $92.0 \pm 4.7\%$ , and that of the UC-MSCs was  $95.5 \pm 2.5\%$  (Fig. S1C). In addition, flow cytometry analysis revealed that the cells expressed positive MSC markers, including CD90 ( $98.8 \pm 0.8\%$  for AD-MSCs and  $99.0 \pm 1.0\%$  for UC-MSCs), CD73 ( $98.6 \pm 0.9\%$  for AD-MSCs and  $98.7 \pm 1.3\%$  for UC-MSCs), and CD105 ( $97.1 \pm 1.7\%$  for AD-MSCs and  $96.1 \pm 1.1\%$  for UC-MSCs), and both expressed low levels of the negative MSC markers CD45, CD34, CD11b, CD19, and HLA-DR ( $0.24 \pm 0.1\%$  for AD-MSCs and  $0.3 \pm 0.2\%$  for UC-MSCs) (Fig. S1D). Taken together, these results indicate that AD-MSCs and UC-MSCs exposed to hypoxic conditions possess the necessary biological properties to be suitable for subsequent experiments.

Characterization of MSC-derived EVs

To calculate the yield of EVs, total EV protein per liter of culture medium was determined using a BCA assay. An average of  $2.27 \pm 0.72$  mg/L AD-MSC-EVs and  $2.05 \pm 0.45$  mg/L UC-MSC-EVs was isolated (Fig. 1A and Table 1). To characterize AD-MSC-EVs and UC-MSC-EVs, the morphology of the EVs was first investigated by TEM. EVs appeared relatively homogeneous as spherical structures with lipid bilayer membranes. The size of the EVs was confirmed by NTA: AD-MSC-EVs was  $186 \pm 131$  nm and UC-MSC-EVs was  $111 \pm 76$  nm in size (Fig. 1B and Table 1). The samples were negative for mycoplasma, bacteria, and fungi (Table 1). Flow cytometry analysis confirmed the expression of the transmembrane proteins CD63 and CD9 in EVs (Fig. 1C and D). AD-MSC-EVs displayed two population of each of CD63 ( $31.5 \pm 9.8\%$  CD63<sup>dim</sup> and  $67.1 \pm 8.9\%$  CD63<sup>bright</sup>) and CD9 ( $56.5 \pm 8.9\%$  CD9<sup>dim</sup> and  $34.2 \pm 5.4\%$  CD9<sup>high</sup>); while there UC-MSC-EVs also showed two populations of CD63 ( $30.5 \pm 2.7\%$  CD63<sup>dim</sup> and  $68.9 \pm 2.7\%$  CD63<sup>bright</sup>), and a single positive CD9 population ( $97 \pm 2.2\%$ ) (Fig. 1C and D, and Table 1).

Growth factors, including BDNF, EGF, FGF-2, HGF, LIF, NGF beta, PDGF-BB, PIGF-1, SCF, VEGF-A and VEGF-D, associated with AD-MSC-EVs and UC-MSC-EVs were evaluated by the Luminex assay. BDNF, NGF beta, PIGF-1, SCF, and VEGF-D were present at very low concentrations ( $< 5$  pg/mg total protein) in both AD-MSC-EVs and UC-MSC-EVs. Although the concentrations of FGF-2, HGF, and LIF in the AD-MSC-EVs were comparable to those in the UC-MSC-EVs, the levels of EGF and VEGF-A in the AD-MSC-EVs were 1.9-fold and 54.5-fold greater, respectively, than those in the UC-MSC-EVs (Fig. 1E and Table 1). PDGF-BB expression was 17-fold greater in the AD-MSCs than in the UC-MSCs, but the difference was not statistically significant. These findings collectively indicate that both types of EVs exhibit biological characteristics in terms of yield, size and morphology consistent with existing nomenclature. Differences were however apparent in that AD-MSC-EVs revealed 2 populations of CD9 (CD9<sup>dim</sup> and CD9<sup>high</sup>), while UC-MSC-EVs had only a CD9<sup>dim</sup> population, and AD-MSC-EVs had higher levels of PDGF-BB and VEGF-A.

The particle concentrations of EV samples were assessed both in freshly prepared and after each three freeze-thaw cycle. The data revealed that a single freeze-thaw cycle did not decrease the particle concentration of either type of EV. However, after two or three freeze-thaw cycles, there was a significant reduction of approximately 40% in the particle concentration for both types of EVs (Fig. 1F). This suggests that repeated freezing and thawing cycles negatively affect the particle concentration of EVs.

EV integrity after 6 months of storage at  $-80\text{ }^{\circ}\text{C}$  was also assessed by evaluating particle concentration, size distribution, protein content, and expression of surface markers CD9 and CD63. Both AD-MSC-EVs and UC-MSC-EVs showed good stability with only minor differences. UC-MSC-EVs retained particle concentration at  $99.2 \pm 0.7\%$ , while AD-MSC-EVs retained  $94.5 \pm 0.7\%$ . A slight increase in particle diameter was observed ( $108.2 \pm 4.5\%$  for UC-MSC-EVs and  $113.2 \pm 3.8\%$  for AD-MSC-EVs). Protein concentration remained stable in

Characteristics		AD-MSC-EVs	UC-MSC-EVs
Yield (mg/L)		$2.27 \pm 0.72$	$2.05 \pm 0.45$
Concentration (particles/ $\mu\text{g}$ of EVs)		$6.7 \times 10^7$	$1 \times 10^8$
Size (nm)		$186 \pm 131$	$111 \pm 76$
CD63 expression (%)	Dim	$31.5 \pm 9.8$	$30.5 \pm 2.7$
	Bright	$67.1 \pm 8.9$	$68.9 \pm 2.7$
CD9 expression (%)	Dim	$56.5 \pm 8.9$	$97 \pm 2.2$
	Bright	$34.2 \pm 5.4$	
Mycoplasma		Negative	Negative
Bacteria and fungi		Negative	Negative
Growth factors (mean $\pm$ SEM) (pg/mg)	EGF	$15.69 \pm 3.15^*$	$8.24 \pm 1.57$
	FGF-2	$122.30 \pm 23.59$	$44.43 \pm 10.93$
	HGF	$300.42 \pm 73.19$	$191.91 \pm 24.84$
	LIF	$19.99 \pm 5.25$	$15.79 \pm 3.49$
	PDGF-BB	$82.88 \pm 61.01$	$4.84 \pm 1.69$
	VEGF-A	$508.17 \pm 93.10^{***}$	$9.33 \pm 1.78$

Table 1. Characterization of human UC-MSC-EVs and AD-MSC-EVs. \* $p < 0.05$ ; \*\*\* $p < 0.001$ ; Student's t test.

both. Surface marker expression was well preserved: AD-MSC-EVs showed  $94.8 \pm 1.2\%$  (CD9) and  $99.8 \pm 0.1\%$  (CD63), while UC-MSC-EVs showed  $98.6 \pm 0.8\%$  and  $99.9 \pm 0.1\%$ , respectively (Fig. S2).

### Vascular and muscular stimulation of UC-MSC-EVs and AD-MSC-EVs

To evaluate whether UC-MSC-EVs and AD-MSC-EVs might induce vascular and muscular stimulation, New Zealand white rabbits were injected with 50  $\mu\text{g}$  of EVs from UC-MSC-EVs or AD-MSC-EVs. Over the next 4 days no rabbits in any group experienced diarrhea, bleeding, edema, purple discoloration, or necrosis. Vascular and muscle stimulation were assessed via HE staining of the injected ears and injected muscles, respectively.

Vascular stimulation test revealed that only one of seven rabbits in the UC-MSC-EV group exhibited mild bruising in the injected ear, which disappeared 96 h post-injection. The temperature of the injected ears measured before and after injection showed no significant difference across all groups (Fig. 2A). Of note, both the Ringer Lactate and AD-MSC-EV animal groups showed a decrease in ear temperature after injection. The change in ear temperature was not therefore related to AD-MSC-EV injection specifically. HE staining of injected ear tissues collected on day 4 post-injection indicated that there was a similar number of blood vessels across all groups (Fig. 2B and G). Blood vessel diameter and area in the injected ear tissues groups injected with either UC-MSC-EVs or AD-MSC-EVs tended to increase when compared animals injected with Ringer Lactate. However, no significant differences in either diameter or area were observed (Fig. 2C,D,G). White blood cells per  $\text{mm}^2$  slightly increased in the ear tissues of the animals injected with UC-MSC-EVs and was greater in the ear tissues of animals injected with AD-MSC-EVs than in those in the Ringer Lactate group ( $p = 0.09$ ) (Fig. 2E). The percentage of lesion area was greater, non-significantly, in the group of rabbits injected with AD-MSC-EVs ( $p = 0.17$ ) and similar between the Ringer Lactate group and the UC-MSC-EVs group (Fig. 2F and G).

The muscular stimulation test revealed that the temperature of the injected muscles was similar before and after infusion with Ringer Lactate, UC-MSC-EVs or AD-MSC-EVs, with no difference between the three analyzed groups (Fig. 2H). HE staining of injected muscles collected on day 4 post-injection indicated that the blood vessel diameters in all groups were similar (Fig. 2I). Rabbits injected with Ringer Lactate and UC-MSC-EVs showed similar percentages of blood vessel areas. Rabbits injected with AD-MSC-EVs tended to show higher level of blood vessel area of injected muscles, but no significant differences among the three groups were observed (Fig. 2J). Collectively, our data indicated that neither UC-MSC-EVs nor AD-MSC-EVs caused vascular or muscular stimulation.

### Systemic hypersensitivity testing of UC-MSC-EVs and AD-MSC-EVs

To investigate whether EVs induce systemic hypersensitivity, New Zealand white rabbits were injected with UC-MSC-EVs or AD-MSC-EVs with doses of either 12.5, 50, or 250  $\mu\text{g}$  on days 0, 2, and 4, and the amount of EVs was doubled on day 14. Groups of rabbits injected with Ringer Lactate or untreated were used as controls (Fig. 3A). During the 14 days of the experiment, the body weight of the injected rabbits gradually increased, and there was no significant difference across analyzed groups (Fig. 3B). A slight decrease in the temperature of the rabbits in all the groups after injection was noted while the temperature remained in the normal range, and no significant difference between the groups was observed (Fig. 3C). No rabbits in any group showed diarrhea, bleeding, edema, purple discoloration, or necrosis. Hematological parameters, including RBC counts, WBC counts, platelet counts, and hemoglobin in the peripheral blood, were investigated before and after each injection. Although the RBC count and hemoglobin level decreased and the platelet number increased after injection, there were no significant differences between the analyzed groups or within groups before and after injection (Fig. 3D–G). These data indicated that neither UC-MSC-EVs nor AD-MSC-EVs significantly changed the hematological indices of the injected rabbits.

Next, the levels of cytokines and factors related to allergies, including histamine and IgE, and the proinflammatory cytokines IL-6, IL-1 $\beta$ , and TNF- $\alpha$  in plasma obtained from blood collected before and after each injection were measured (Fig. 4). It is found that the level of histamine transiently increased after injection of both medium and high doses of UC-MSC-EVs and AD-MSC-EVs, although the difference was not statistically significant. The Ringer Lactate-injected groups also showed a slight increase in histamine levels after the three first injections and a return to the starting level after the 4th injection. Histamine levels following high dose injection of UC-MSC-EVs and AD-MSC-EVs increased after the 1st injection, peaked after the 2nd injection and gradually decreased after the 3rd and 4th injections (Fig. 4A). The IgE levels were similar between the groups before and after injection (Fig. 4B). Most of the injected animals did not show induction of the proinflammatory cytokines IL-6, IL-1 $\beta$ , and TNF- $\alpha$  (Fig. 4C–E).

### Acute toxicity testing of UC-MSC-EVs and AD-MSC-EVs

To examine whether EVs cause acute toxicity, Swiss mice ( $n = 6$ ) were intravenously injected with UC-MSC-EVs or AD-MSC-EVs at different doses (500, 2000, 5000, or 10000  $\mu\text{g}/\text{kg}$  of body weight). A group of mice ( $n = 6$ ) intravenously injected with Ringer Lactate was used as a control. The acute toxicity of the EVs was determined by monitoring body weight and survival for 14 days after injection (Fig. 5A). The body weight of the injected mice gradually increased after injection (Fig. 5B and D). With 100% of the mice survival across all the analyzed groups, the  $\text{LD}_{50}$  could not be calculated (Fig. 5C and E). These results suggested that even the highest dose of 10,000  $\mu\text{g}/\text{kg}$  of body weight (equivalent to a dose of  $8.4 \times 10^{10}$  particles for UC-MSC-EVs or  $5.8 \times 10^{10}$  particles for AD-MSC-EVs per kg of body weight in humans) was not lethal to mice.

### Subchronic toxicity testing of UC-MSC-EVs and AD-MSC-EVs

To examine whether UC-MSC-EVs and AD-MSC-EVs induce subchronic toxicity, Wistar rats ( $n = 6$ ) were intravenously injected 3 times at 10-day intervals with low (50  $\mu\text{g}$ ) or high (150  $\mu\text{g}$ ) doses of UC-MSC-EVs or AD-MSC-EVs (Fig. 6A). The body weight of the injected rats was maintained throughout the experiment,

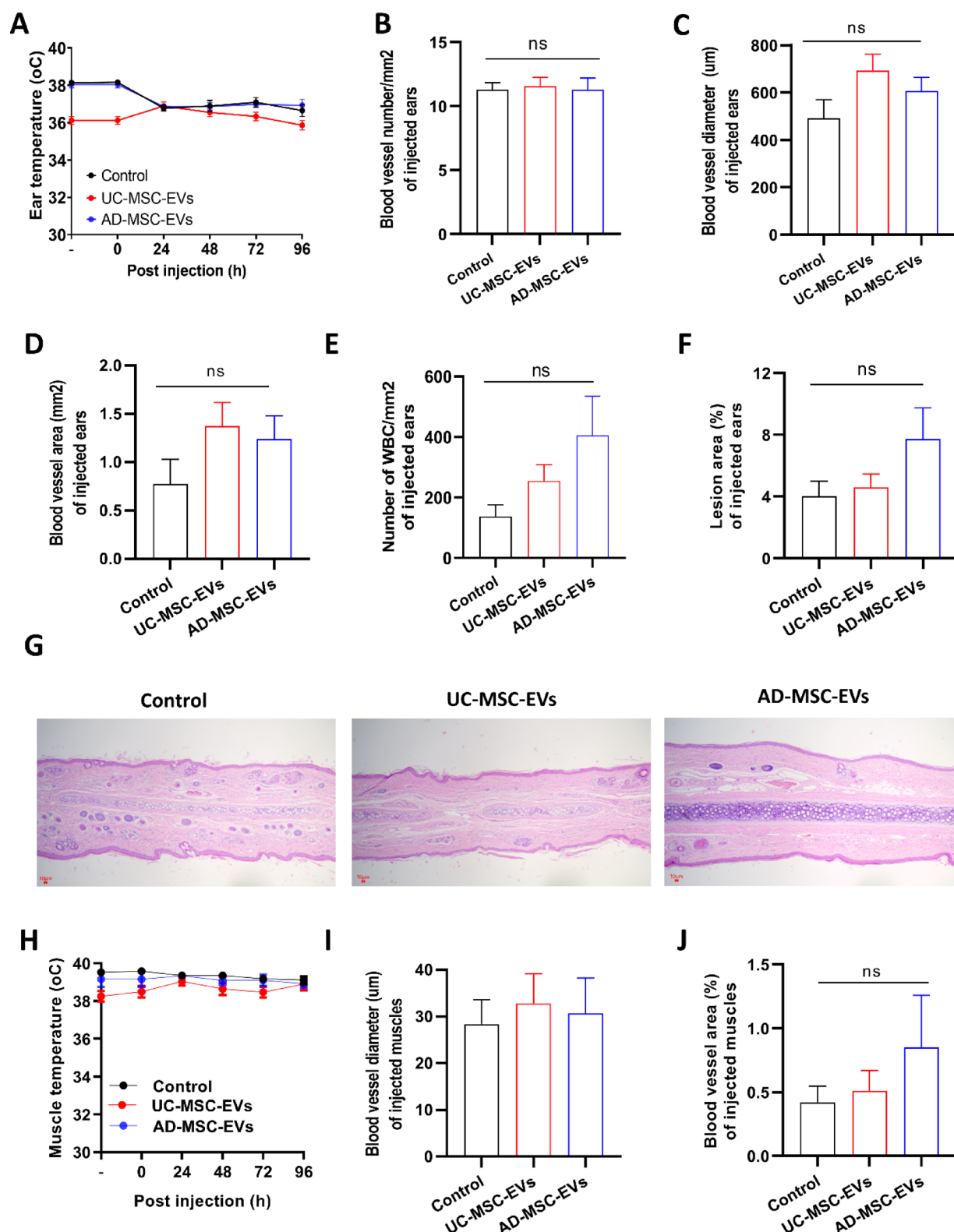


**Fig. 2.** Vascular and muscular stimulation of UC-MSC-EVs and AD-MSC-EVs. New Zealand rabbits were injected with either Ringer Lactate (control), 50  $\mu$ g of UC-MSC-EVs, or 50  $\mu$ g of AD-MSC-EVs. **(A)** The temperatures of the injected ears were measured at the indicated time points. **(B–G)** HE staining of injected ears on day 4 post-injection to evaluate vascular stimulation, including the number of blood vessels per mm<sup>2</sup> (B), blood vessel diameter (C), blood vessel area (D), number of WBCs (E), percentage of lesion area (F), and representative HE staining of injected ears (G). **(H)** The temperatures of the injected muscles were measured at the indicated time points. **(I–J)** HE staining analysis of injected muscle on day 4 post-injection to measure the blood vessel diameter (I) and percentage of lesion area (J). The data are presented as mean  $\pm$  SEM. Significant differences between groups were analyzed by ANOVA/Bonferroni. Ns indicate not significant.



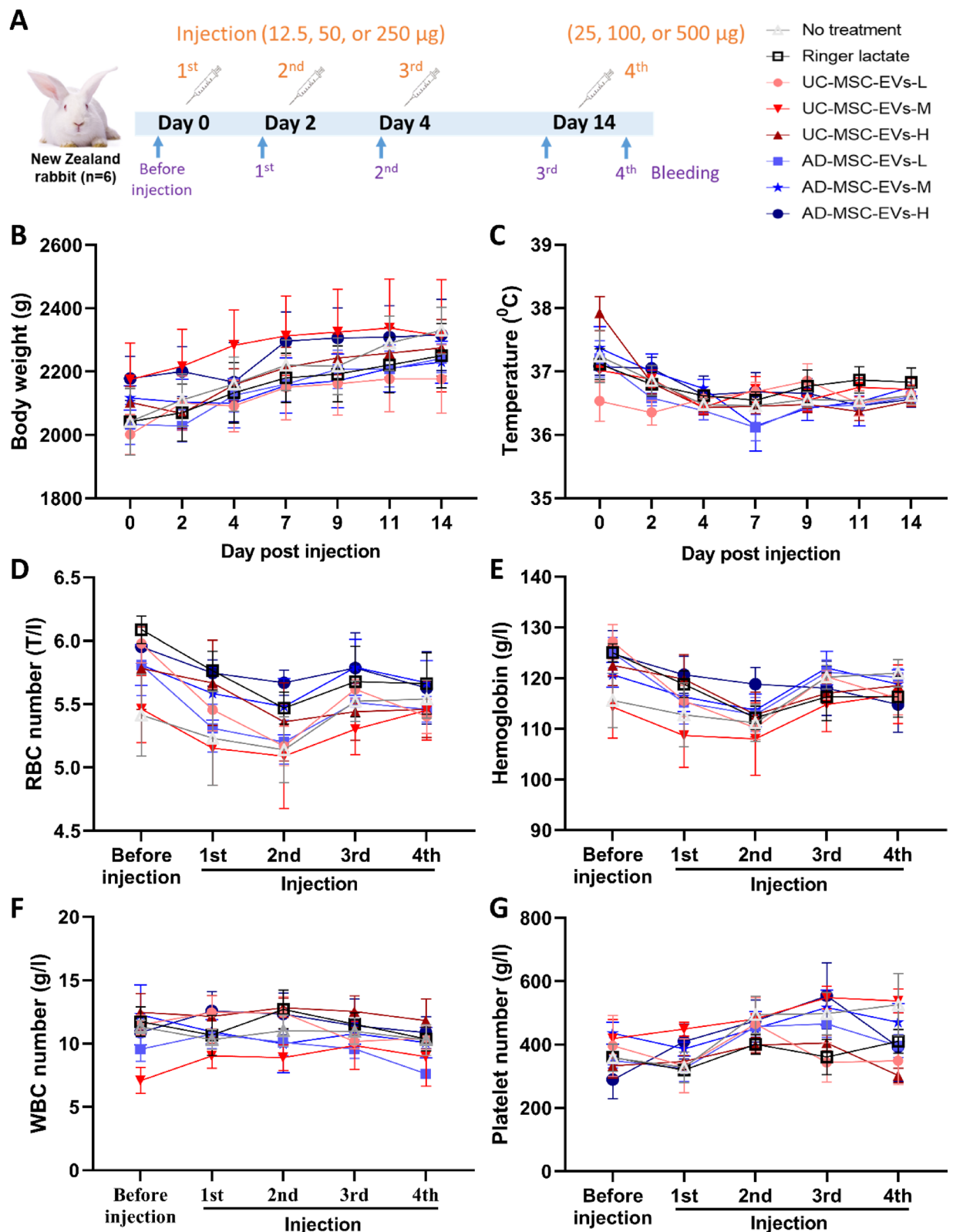


**Fig. 3.** Systemic hypersensitivity effects of UC-MSC-EVs and AD-MSC-EVs. New Zealand rabbits ( $n=6$ ) were injected with either Ringer Lactate, UC-MSC-EVs or AD-MSC-EVs at low (12.5  $\mu$ g), medium (50  $\mu$ g), or high (250  $\mu$ g) doses on days 0, 2, and 4. On day 14, the injected doses were doubled in the respective groups. Groups injected with Ringer Lactate or untreated were used as controls. (A) The experimental scheme. The body weight (B) and temperature (C) of the injected animals were monitored for 14 days. RBC counts (D), hemoglobin (E), WBC counts (F), and platelet counts (G) in the peripheral blood were determined before and after each injection. The data are presented as mean  $\pm$  SEM.



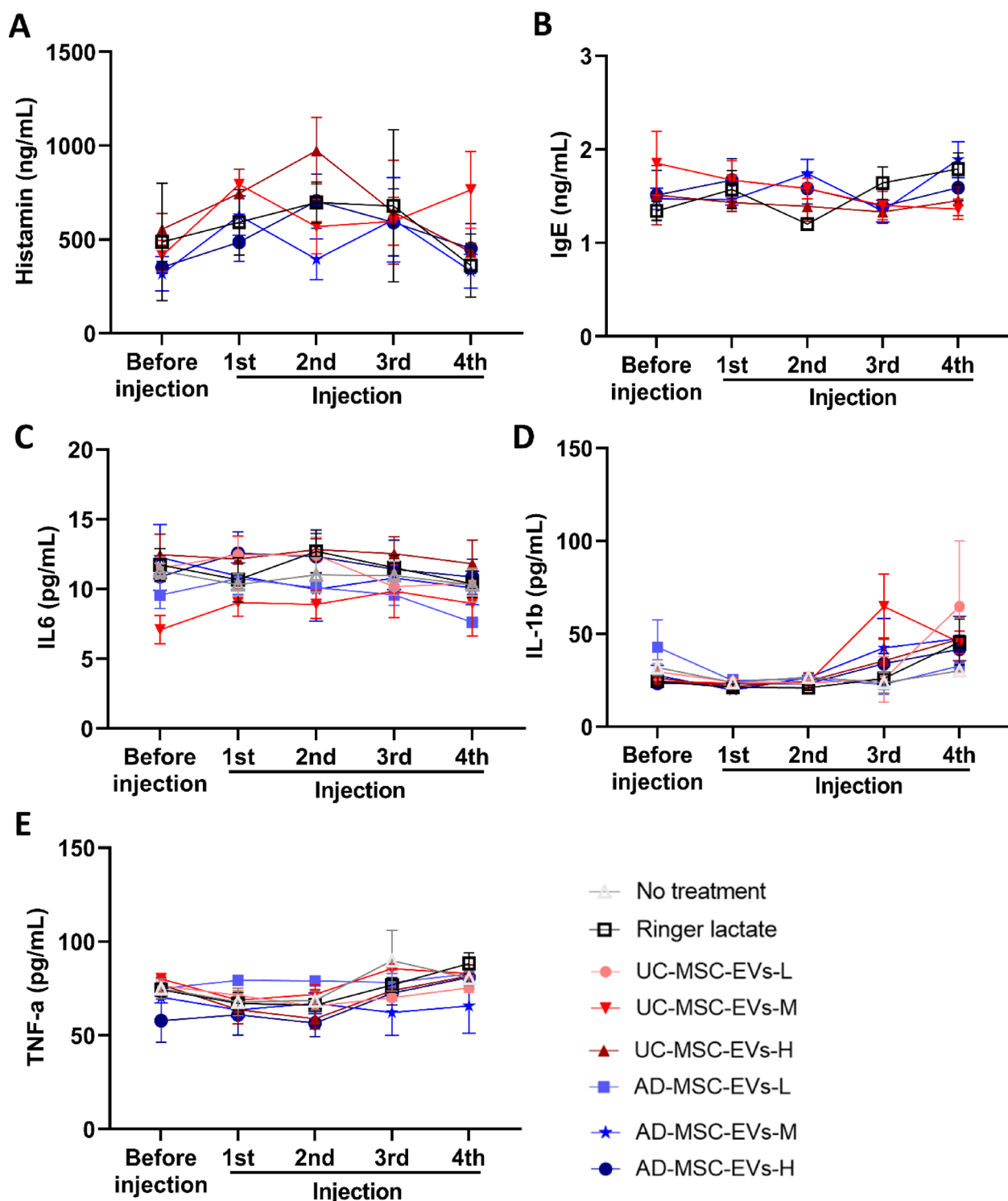


**Fig. 4.** UC-MSC-EVs and AD-MSC-EVs did not induce allergy- or systemic inflammation-related reactions after injection. New Zealand rabbits ( $n=6$ ) were injected with either Ringer Lactate, UC-MSC-EVs or AD-MSC-EVs at low, medium or high doses on days 0, 2, 4, and 14. No treatment was used as a control. Blood was collected before the 1st injection, 2 days after the 1st and 2nd injections, 10 days after the 3rd injection, and 30 min after the 4th injection. Plasma levels of histamine (A), IgE (B), IL-6 (C), IL-1 $\beta$  (D), and TNF- $\alpha$  (E) were measured by ELISA. The data are presented as mean  $\pm$  SEM.

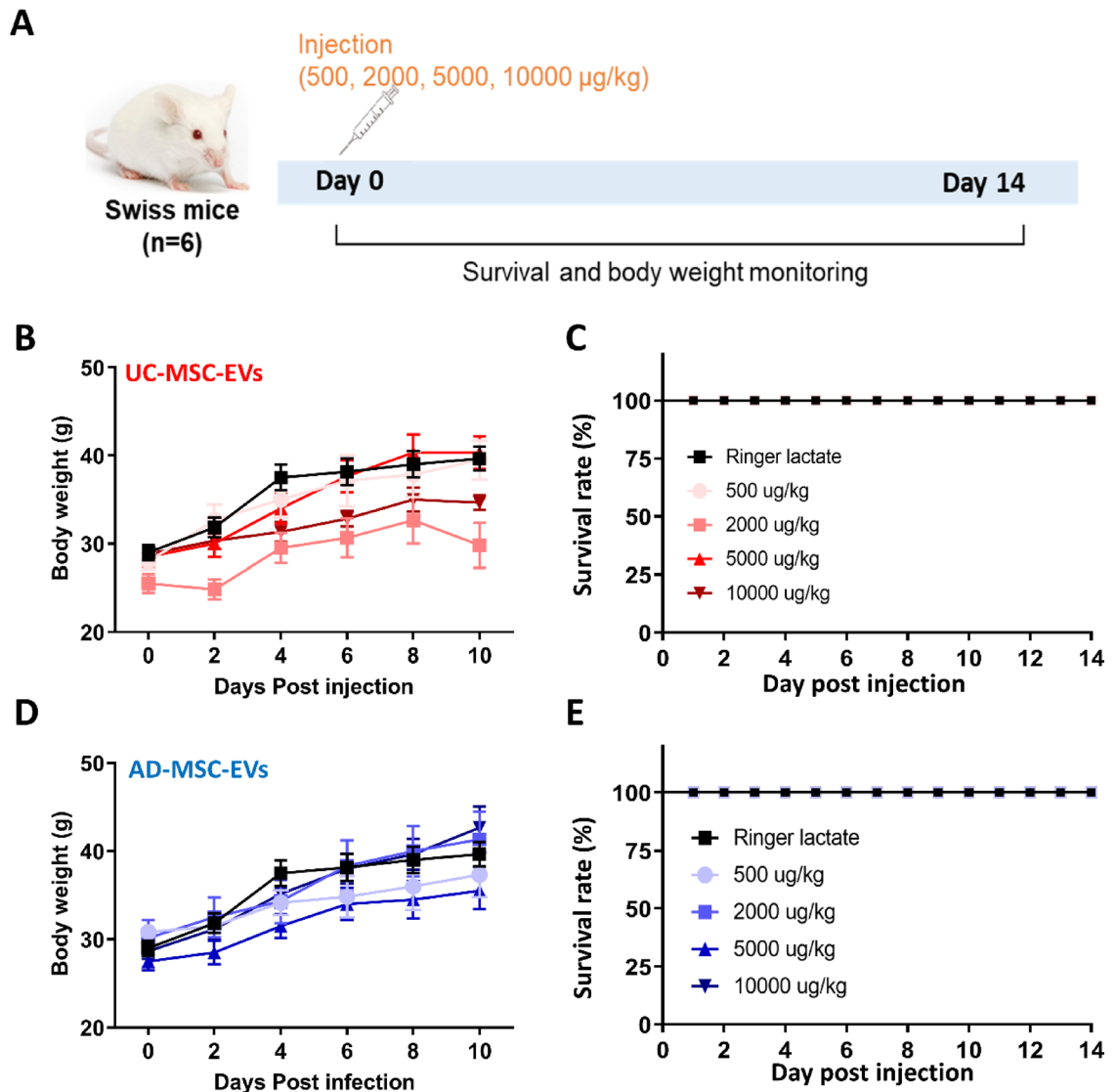


**Fig. 5.** Acute toxicity of UC-MSC-EVs and AD-MSC-EVs. Swiss mice ( $n=6$ ) were injected with UC-MSC-EVs or AD-MSC-EVs at different doses and compared to those injected with Ringer Lactate. **(A)** The experimental scheme. **(B–E)** Body weight (**B** and **D**) and the survival rate (**C** and **E**) were monitored for 14 days. The data are presented as mean  $\pm$  SEM.

suggesting that the injection of UC-MSC-EVs or AD-MSC-EVs did not affect the body weight of the animals (Fig. 6B). The blood cell counts before and after 10 days of each injection indicated that neither UC-MSC-EVs nor AD-MSC-EVs changed the hematological indices, including the number of WBCs (Fig. 6C), the number of RBCs (Fig. 6D), hemoglobin levels (Fig. 6E), and the number of platelets (Fig. 6F), of the injected rats. The levels of AST and ALT (Fig. 7A) and urea and creatinine (Fig. 7B) in the blood of rats were similar before and after injection in all analyzed groups. Histological examination of the liver, kidney, and spleen of injected rats ( $n=3$ ) on day 30 after the first injection revealed no macroscopic pathological changes. Microscopic observation indicated that there were no significant differences in the microscopic structures of the liver, kidney or spleen before and after treatment or between groups (Fig. 7C). Taken together, these data indicate that neither UC-MSC-EVs nor AD-MSC-EVs led to subchronic toxicity in rat.

## Discussion

EVs have attracted significant attention in the field of regenerative medicine due to their diversity of potential applications. These nanoscale, membrane-bound vesicles are secreted by a wide range of cell types, including MSCs, and have demonstrated potential in promotion of tissue repair and regeneration. Hypoxia preconditioning has been considered a strategy to improve the function of MSC-derived EVs. In this study, EVs were isolated from AD-MSCs and UC-MSCs that were cultured for 3 days under 21% oxygen and then primed them with 5% oxygen for 2 days. Our isolated EVs exhibited the size and morphology, consistent with a previous study showing that physiological oxygen levels (5%) did not change the size of EVs secreted by AD-MSCs compared

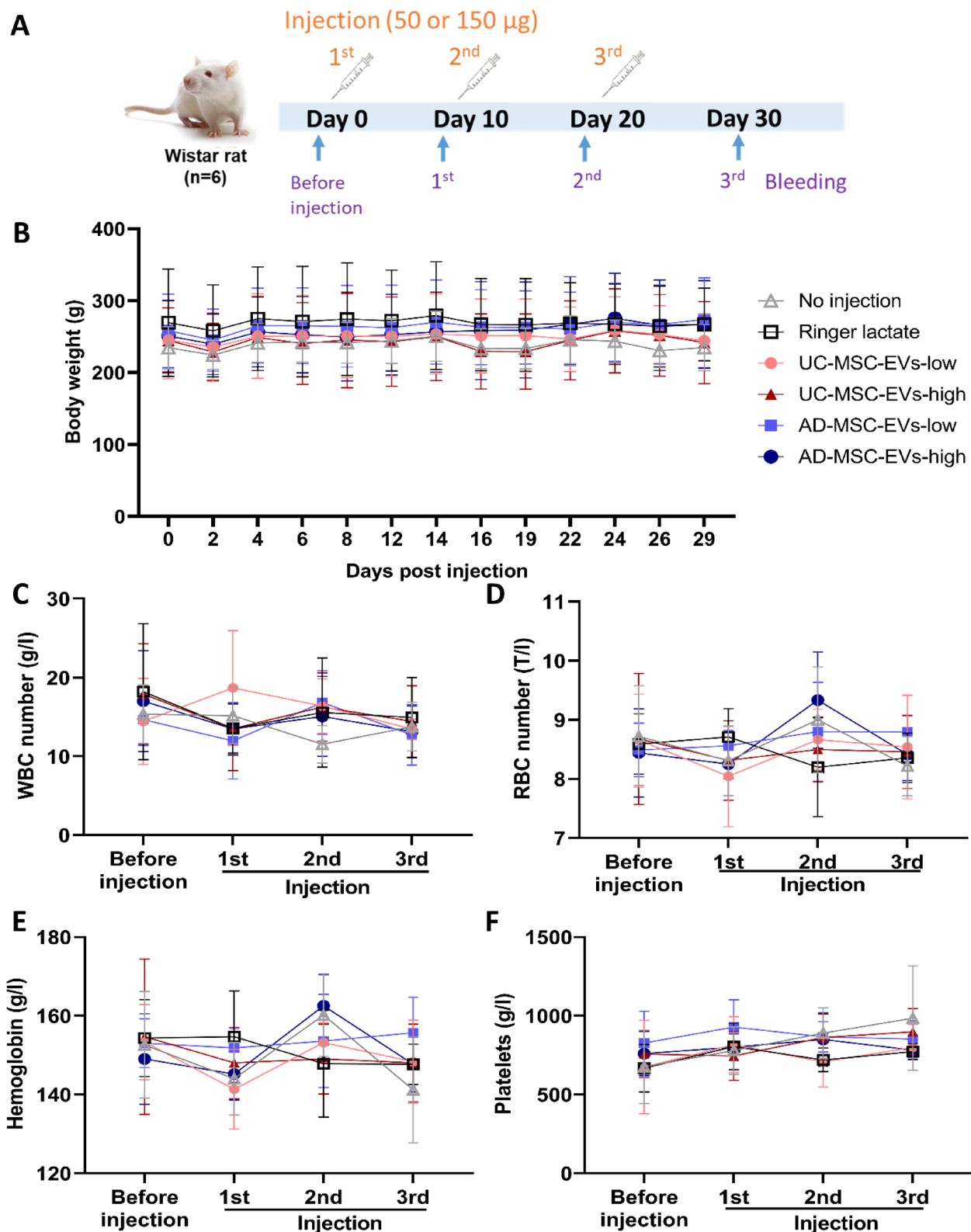


**Fig. 6.** Effects of UC-MSC-EVs and AD-MSC-EVs on hematological indices of rats. Wistar rats were injected with either Ringer Lactate, UC-MSC-EVs or AD-MSC-EVs at low (50  $\mu$ g) or high doses (150  $\mu$ g) on days 0, 10, and 20. Groups of rats injected with Ringer Lactate or untreated were used as controls. **(A)** The experimental scheme. **(B)** The body weights of the injected animals were monitored for 29 days. **(C–F)** The number of WBCs (C), number of RBCs (D), hemoglobin levels (E), and number of platelets (F) in blood collected before and 10 days after each injection were determined. The data are presented as mean  $\pm$  SEM.



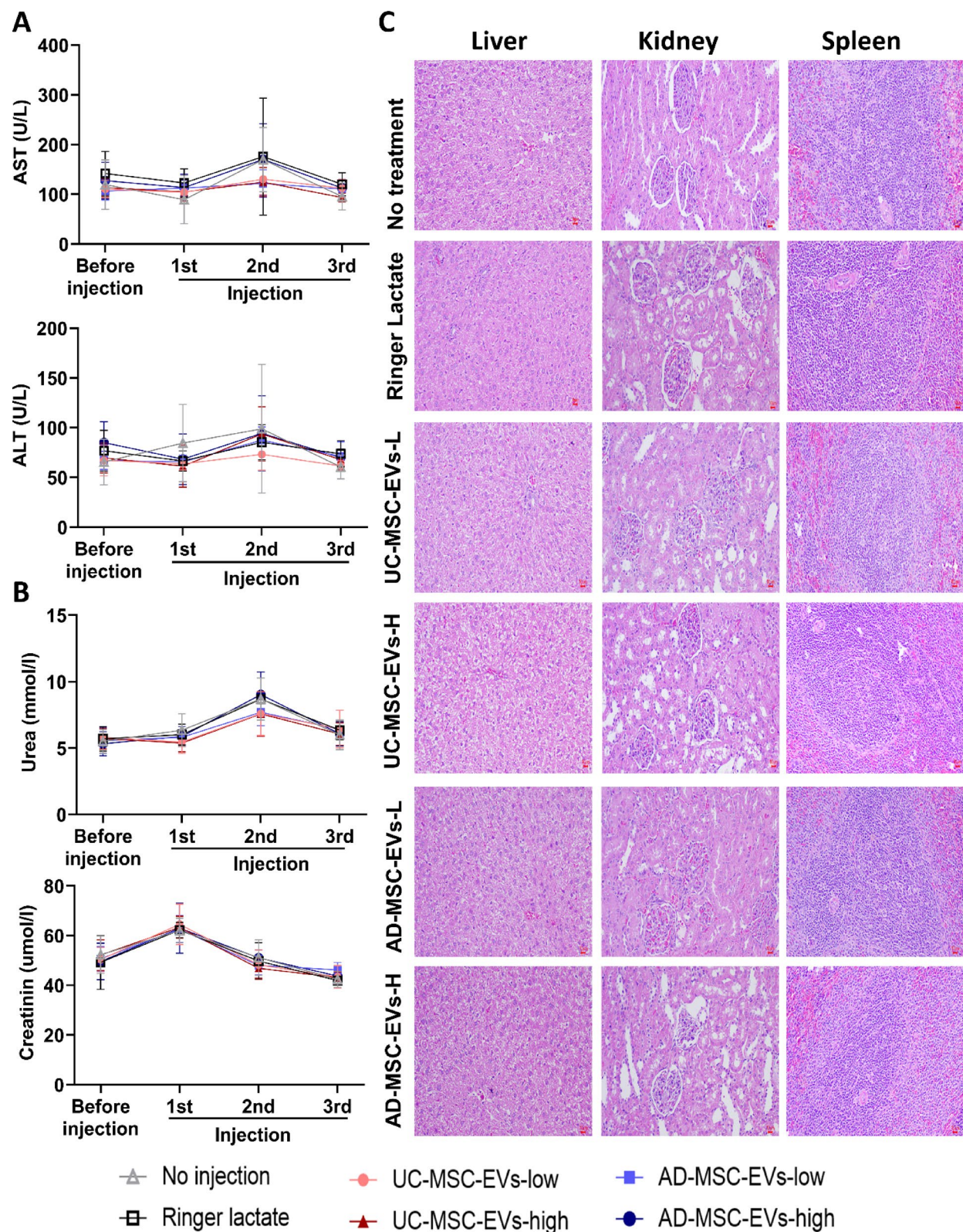


**Fig. 7.** UC-MSC-EVs and AD-MSC-EVs administration does not damage the liver, kidney, or spleen. Wistar rats were injected with either Ringer Lactate, UC-MSC-EVs or AD-MSC-EVs at low (50  $\mu$ g) (UC-MSC-EVs-L and AD-MSC-EVs-L, respectively) or high (150  $\mu$ g) (UC-MSC-EVs-H and AD-MSC-EVs-H, respectively) doses on days 0, 10, and 20. The levels of AST and ALT (A) and urea and creatinine (B) in blood collected before and 10 days after each injection were measured. On day 30 post-injection, the liver, kidney, and spleen were collected for macroscopic and microscopic observation via H&E staining (C). The data are presented as mean  $\pm$  SEM.

to those secreted by EVs cultured in ambient oxygen<sup>26</sup>. The classical tetraspanins CD9 and CD63, which are commonly present in EVs<sup>27</sup>, were also highly expressed on both AD-MSC-EVs and UC-MSC-EVs. Notably, AD-MSC-EVs had two populations with different CD9 expression, CD9<sup>dim</sup> and CD9<sup>bright</sup>, while UC-MSC-EVs expressed only one CD9<sup>+</sup> population. These findings suggest that MSC-derived EVs are heterogeneous and include several subsets with different phenotypes. However, the characteristics and clinical potential of each subset remain unclear.

Importantly, the isolated EVs released high levels of growth factors, including EGF, FGF-2, HGF, LIF, PDGF-BB, and VEGF-A, which are related to angiogenesis and regenerative capacity. Previous data consistent with our ours demonstrated that EVs secreted by hypoxia-primed MSCs released higher VEGF than those from MSCs cultured under normoxic air oxygen<sup>22,26</sup>. Interestingly, EVs from AD-MSCs produced EGF, FGF-2, PDGF-BB, and VEGF-A at higher levels than EVs from UC-MSCs under hypoxic conditions. This is consistent with a previous study showing that EVs from AD-MSCs had higher levels of FGF-2, HGF, and VEGF-A than those from UC-MSCs<sup>28</sup>. Our data also indicated that more than two freeze–thaw cycles led to a reduction in particle concentration for both types of EVs. This finding is consistent with previous reports showing that repeated freeze–thawing can decrease EV concentration and bioactivity, while increasing particle size and aggregation<sup>29</sup>. Future studies should evaluate the stability of additional EV cargo, such as growth factors, following multiple freeze–thaw cycles to better characterize the functional consistency and therapeutic potential of EV preparations. The stability of both AD-MSC-EVs and UC-MSC-EVs was assessed after 6 and 10 months of storage at  $-80^{\circ}\text{C}$ , respectively. The EVs retained particle concentration and surface marker expression (CD9 and CD63) with only minor changes. A slight increase in particle diameter was observed, while protein concentration remained stable. These findings are consistent with previous reports showing that EVs stored at  $-80^{\circ}\text{C}$  generally retain size, concentration, surface markers, and bioactivity for months, and stabilizers like trehalose or sucrose can help preserve their integrity during storage<sup>29</sup>. Collectively, our results are consistent with previous studies showing that EVs secreted by hypoxia-primed MSCs exhibit typical characteristics of EVs in terms of morphology, size, marker expression and growth factor profiles. In addition, the differential features of EVs from AD- and UC-MSCs was also highlighted. Further investigation is needed to determine whether these differences may influence the therapeutic potential of these cells. Importantly, while several studies have demonstrated the benefits of EVs derived from MSCs cultured under hypoxic conditions *in vitro*, *in vivo* data are still lacking. Therefore, it is necessary to address this gap by comprehensively investigating the safety profile of EVs derived from hypoxia-primed AD-MSCs and UC-MSCs in animal models before considering their implementation in human research.

Safety evaluation using small animals, such as mice and rabbits, plays a crucial role in the drug development process<sup>24,30</sup>. Herein, the safety profile of our isolated EVs, including local (vascular or muscular) stimulation, systemic hypersensitivity, acute toxicity, and subchronic toxicity, was rigorously tested at varying protein-based doses, a practical and commonly used approach in preclinical models. However, due to variability in particle-to-protein ratios between EV sources, particle numbers were also considered and discussed for future dosing standardization. Our vascular and muscular stimulation test in rabbits revealed that, similar to the control animal group, injection of EVs at a dose of  $50\text{ }\mu\text{g}$  per animal (approximately  $5 \times 10^9$  particles for UC-MSC-EVs and  $3.5 \times 10^9$  particles for AD-MSC-EVs) had no effect on the temperature of the injection sites, whether in the ears or muscles. During the experiments, there were no adverse events, including bleeding, redness, swelling, or necrosis at the injected sites, except for one rat of UC-MSC-EVs group with temporary mild bruising (commonly reported after intravenous administration) in the injected ears, which disappeared at 96 h post-injection. Although minor changes in the diameter and area of blood vessels were observed following the administration of EVs, the number of blood vessels was similar in all the tested groups. The number of infiltrating WBCs in the injection area was the greatest in the AD-MSC-EV group, followed by the UC-MSC-EV group, and the lowest in the Ringer Lactate injected group. Correspondingly, animals injected with AD-MSC-EVs showed a slight increase in lesion area. However, there was no significant difference in the analyzed parameters among the groups. This result suggested that the injection of EVs from AD-MSCs and UC-MSCs might induce mild local immune responses, especially in the former group. Overall, our data demonstrated that EVs from both hypoxia-primed AD-MSCs and UC-MSCs can be applied through vascular and muscular routes without significant vascular or muscular stimulation in the tested animals. This finding is consistent with a study by Sun et al. that showed that there was no vascular or muscular stimulation following the administration of exosomes derived from human MSCs in rabbits<sup>31</sup>.

In addition to local stimulation testing, the potential of EVs to induce systemic anaphylaxis was examined through repeated injections in rabbits at doses of 12.5, 50, and  $250\text{ }\mu\text{g}$  per animal -corresponding to approximately  $1.25 \times 10^9$ ,  $5 \times 10^9$ , and  $2.5 \times 10^{10}$  particles for UC-MSC-EVs, and  $8.63 \times 10^8$ ,  $3.5 \times 10^9$ , and  $1.7 \times 10^{10}$  particles for AD-MSC-EVs, respectively. Injections were administered three times at 2-day intervals, followed by a double-dose challenge one week after the third injection. No adverse events, including bleeding, redness, edema, purple discoloration, or necrosis, occurred after the injections, except for 3 rabbits that showed diarrhea after the injections which recovered after 2–4 days of treatment with biseptol. It was observed that rabbits were highly sensitive to quarantine conditions and often experienced diarrhea. Notably, five rabbits in the experimental set had diarrhea before the experimental initiation. Therefore, the observed diarrhea was attributed to the model conditions rather than the administered treatment. While the body weight of the injected animals gradually increased post-injection, the temperature of the animals varied at baseline and was comparable between the analyzed groups at later time points. The number of RBCs and hemoglobin levels tended to decrease after the first and second treatments in all groups but subsequently normalized. Injection of EVs has been reported to decrease RBC and hemoglobin levels in a pig model of spinal cord injury<sup>32</sup>. A similar tendency was observed in both the Ringer Lactate and untreated groups in this study, suggesting that the change reflects a normal physiological response in the studied animals. While the WBC number was maintained during the experiment,



the platelet number slightly increased in some EV groups, similar to that in untreated animals. Histamine and IgE are important markers related to allergic reactions. MSCs have been demonstrated to reduce the blood level of histamine in rats with allergic rhinitis<sup>33</sup>. In this study, the 1st and 2nd injections of high-dose EVs into healthy rabbits induced a transient increase in serum histamine levels, but the serum histamine levels returned to the normal baseline despite of the injection of two additional doses. Notably, Ringer Lactate injection also had a similar effect. Furthermore, IgE levels remained stable at all analyzed time points in all groups. Repeated administration of EVs did not elicit significant changes in the levels of proinflammatory cytokines, including IL-6, IL1 $\beta$ , and TNF- $\alpha$ . Taken together, these findings show that repeated injections of up to 250  $\mu$ g of AD-MSC-EVs or UC-MSC-EVs did not trigger allergic reactions in healthy rabbits.

Although acute toxicity studies are commonly conducted to determine the short-term adverse effects of a drug<sup>34</sup>, to our knowledge, no published studies have reported this type of evaluation for EVs. Therefore, in the present study, acute toxicity testing was assessed through single intravenous infusion in mice, with various doses of EVs (500, 2000, 5000, and 10,000  $\mu$ g/kg body weight, corresponding to approximately  $5 \times 10^{10}$ ,  $2 \times 10^{11}$ ,  $5 \times 10^{11}$ , and  $1 \times 10^{12}$  particles for UC-MSC-EVs, and  $3.5 \times 10^{10}$ ,  $1.4 \times 10^{11}$ ,  $3.5 \times 10^{11}$ , and  $6.9 \times 10^{11}$  particles for AD-MSC-EVs). The body weight of the injected animals increased slightly, while no changes in behavior were noted. Additionally, EV treatment at doses up to 10,000  $\mu$ g/kg body weight had no short-term effects on the survival of the tested mice. A previous study showed that the median EV dose used for mice, based on 50 different preclinical studies, was 7,500  $\mu$ g/kg of body weight, while the EV dose for humans to treat several diseases ranged from  $2 \times 10^8$  to  $2 \times 10^{10}$  particles<sup>35</sup>. Herein, our established safe dose was more than 10,000  $\mu$ g/kg of body weight for mice, equivalent to a human dose of  $8.4 \times 10^{10}$  particles for UC-MSC-EVs or  $5.8 \times 10^{10}$  particles for AD-MSC-EVs per kg of body weight (the human dose was calculated by multiplying the mouse dose by 0.081, as described previously<sup>36</sup>. Our results might provide an important reference for safe EV doses for other preclinical and clinical investigations.

Finally, a subchronic toxicity test was conducted to assess whether EVs induce long-term toxicity in animals. In agreement with previously published data<sup>37,38</sup>, our results showed that intravenous injection of 50–150  $\mu$ g of EVs (equal to  $5 \times 10^9$  or  $1.5 \times 10^{10}$  particles for UC-MSC-EVs and  $3.45 \times 10^9$  or  $1.04 \times 10^{10}$  particles for AD-MSC-EVs) three times with a 10-day interval did not induce long-term toxicity in rats. There were no adverse events, bleeding, redness, edema, purple discoloration, or necrosis after injection. The complete blood count results indicated that there were no significant differences in the WBC, RBC, and platelet counts or hemoglobin levels, suggesting that there were no significant effects on hematological parameters after EV injection. Administration of AD-MSCs and UC-MSCs did not affect the serum levels of liver (AST and ALT) or kidney (urea and creatinine) functional markers or lead to histopathological changes in the liver, kidney, or spleen of the injected animals. Previously reported data showed that intravenous injection of Expi293F-derived EVs ( $5 \times 10^{10}$  EV particles per animal) into mice did not result in any histopathological changes or increases in liver transaminase levels<sup>38</sup>. In addition, Rodrigues et al. showed that administration of repeated doses of UC-MSC-EVs to rats for 6 weeks or 12 weeks, for a total of  $1 \times 10^{11}$  EV particles, did not affect blood cell counts or kidney or liver toxicity<sup>37</sup>. Injection of 400–800  $\mu$ g of UC-MSC-EVs did not significantly change liver function indices, including AST, ALT, alkaline phosphatase (ALP), total cholesterol (TCH), total protein (TP), albumin (ALB), and renal function indices, such as blood urea nitrogen and creatinine, in Sprague–Dawley rats<sup>31</sup>. Overall, our long-term investigation of EV administration suggested that EVs had no significant side effects on important organs and tissues, such as the liver, kidney, and spleen, in rats. One limitation of this study is the absence of organ weight measurements, which could have provided additional insights into subtle organ-specific toxicities. Further analysis of additional organs, such as the heart and lungs, may also help to establish a more comprehensive safety profile in future studies.

Collectively, our data indicated that our EVs, which were isolated from UC-MSCs and AD-MSCs, cultured in xeno- and serum-free medium and primed with 5% oxygen, did not cause local (vascular or muscular) stimulation, systemic hypersensitivity, or short- or long-term toxicity in the tested animals. While the data suggest that EVs are safe in healthy small animals, several questions remain regarding the safe dose of EVs in larger animals, the safety of EVs in experimental disease models, and the *in vivo* kinetics and biodistribution of EVs. Addressing these questions will further elucidate the safety of MSC-derived EVs for clinical use, paving the way for successful translation to human studies.

## Conclusion

In this study, we successfully isolated EVs from UC-MSCs and AD-MSCs cultured in xeno- and serum-free media and primed with 5% oxygen. Our study is the first to evaluate the safety of the EVs using animals. Overall, our results confirm the safety of both UC-MSCs and AD-MSCs in rabbits and rodents (Fig. 8). Additionally, we believe that the comprehensive approach employed in our study will provide other researchers with a framework to assess the immunogenicity and toxicity of their EVs, facilitating the development of therapeutic EVs for various disease models and human studies.

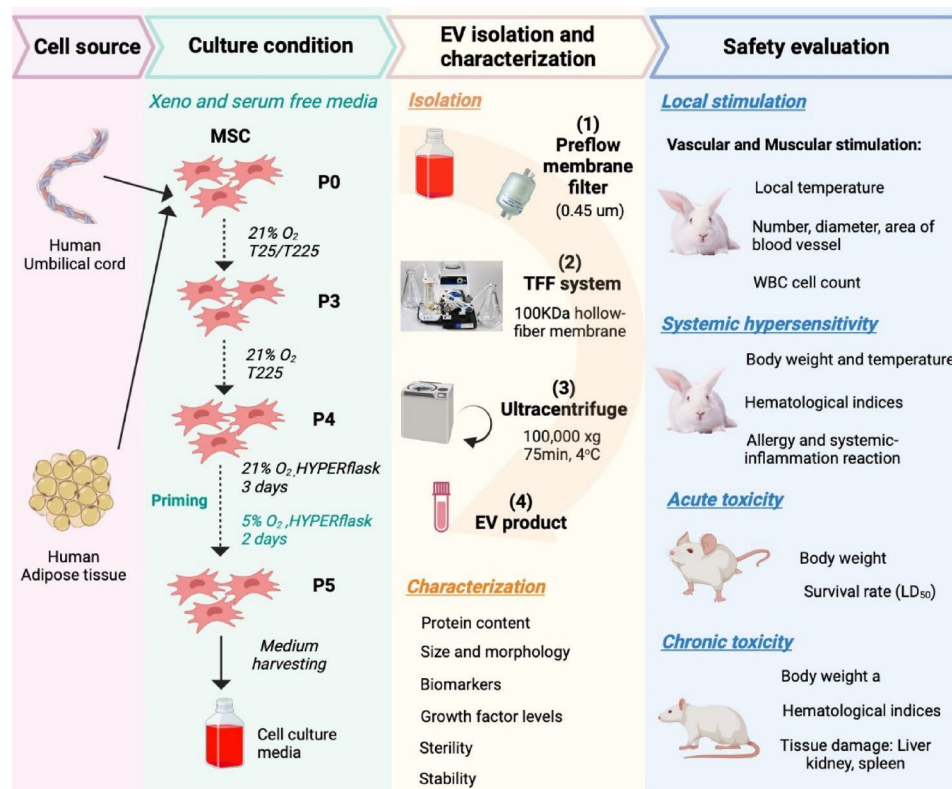


**Fig. 8.** Schematic overview of the EV safety evaluation workflow. MSCs from human umbilical cord and adipose tissue were expanded in xeno-/serum-free media and primed under hypoxic conditions. EVs were isolated and characterized by assessing protein content, size, markers, growth factors, sterility, and stability. Safety of UC-MSC-EVs and AD-MSC-EVs was assessed through: (1) local stimulation in rabbits; (2) systemic hypersensitivity in rabbits; (3) acute toxicity in mice and (4) subchronic toxicity in rats.

## Data availability

The authors confirm that the data supporting the findings of this study are available within the article and its supplementary materials.

Received: 25 February 2025; Accepted: 12 September 2025

Published online: 16 October 2025

## References

- Yáñez-Mó, M. et al. Biological properties of extracellular vesicles and their physiological functions. *J. Extracell. Ves.* **4**(1), 27066 (2015).
- Mathieu, M. et al. Specificities of secretion and uptake of exosomes and other extracellular vesicles for cell-to-cell communication. *Nat. Cell Biol.* **21**(1), 9–17 (2019).
- Vizoso, F. J., Eiro, N., Cid, S. & Schneider, J. Mesenchymal stem cell secretome: toward cell-free therapeutic strategies in regenerative medicine. *Int. J. Mol. Sci.* **18**(9), 1852 (2017).
- Kalluri, R. et al. The biology, function, and biomedical applications of exosomes. *Science* **367**(6478), eaau6977 (2020).
- Van Niel, G. et al. Shedding light on the cell biology of extracellular vesicles. *Nat. Rev. Mol. Cell Biol.* **19**(4), 213–228 (2018).
- Ding, D.-C. & Shyu, W.-C. Mesenchymal stem cells. *Cell Transplant.* **20**(1), 5–14 (2011).
- Pittenger, M. F. et al. Multilineage potential of adult human mesenchymal stem cells. *Science* **284**(5411), 143–147 (1999).
- English, K. J. I. Mechanisms of mesenchymal stromal cell immunomodulation. *Immunol. Cell Biol.* **91**(1), 19–26 (2013).
- Hazrati, A. et al. Mesenchymal stromal/stem cells and their extracellular vesicles application in acute and chronic inflammatory liver diseases: emphasizing on the anti-fibrotic and immunomodulatory mechanisms. *Front. Immunol.* **13**, 865888 (2022).
- Sohrabi, B. et al. Mesenchymal stem cell (MSC)-derived exosomes as novel vehicles for delivery of miRNAs in cancer therapy. *Cancer Gene Ther.* **29**(8–9), 1105–1116 (2022).
- Ferreira, J. R. et al. Mesenchymal stromal cell secretome: influencing therapeutic potential by cellular pre-conditioning. *Front. Immunol.* **9**, 2837 (2018).
- Cunningham, C. J. et al. The therapeutic potential of the mesenchymal stem cell secretome in ischaemic stroke. *J. Cerebr. Blood Flow Metab.* **38**(8), 1276–1292 (2018).
- Harrell, C. R. et al. Molecular mechanisms responsible for therapeutic potential of mesenchymal stem cell-derived secretome. *Cells* **8**(5), 467 (2019).
- Hade, M. D., Suire, C. N. & Suo, Z. J. C. Mesenchymal stem cell-derived exosomes: applications in regenerative medicine. *Cells* **10**(8), 1959 (2021).
- Vatsa, P., Negi, R., Ansari, U., Khanna, V. & Pant, A. J. M. N. Insights of extracellular vesicles of mesenchymal stem cells: a prospective cell-free regenerative medicine for neurodegenerative disorders. *Mol. Neurobiol.* **59**, 1–16 (2022).

16. Grayson, W. L. et al. Effects of hypoxia on human mesenchymal stem cell expansion and plasticity in 3D constructs. *J. Cell. Physiol.* **207**(2), 331–339 (2006).
17. Fehrer, C. et al. Reduced oxygen tension attenuates differentiation capacity of human mesenchymal stem cells and prolongs their lifespan. *Aging Cell* **6**(6), 745–757 (2007).
18. D'Ippolito, G., Diabira, S., Howard, G. A., Roos, B. A. & Schiller, P. C. J. B. Low oxygen tension inhibits osteogenic differentiation and enhances stemness of human MIAMI cells. *Bone* **39**(3), 513–522 (2006).
19. Basciano, L. et al. Long term culture of mesenchymal stem cells in hypoxia promotes a genetic program maintaining their undifferentiated and multipotent status. *BMC Cell Biol.* **12**(1), 1–12 (2011).
20. Liu, W. et al. Hypoxic mesenchymal stem cell-derived exosomes promote bone fracture healing by the transfer of miR-126. *Acta Biomater.* **103**, 196–212 (2020).
21. Braga, C. L. et al. Proteomics profile of mesenchymal stromal cells and extracellular vesicles in normoxic and hypoxic conditions. *Cytotherapy* **24**(12), 1211–1224 (2022).
22. Phelps, J. et al. Physiological oxygen conditions enhance the angiogenic properties of extracellular vesicles from human mesenchymal stem cells. *Stem Cell Res. Therapy.* **14**(1), 218 (2023).
23. Dessels, C. et al. Making the switch: alternatives to fetal bovine serum for adipose-derived stromal cell expansion. *Front. Cell Dev. Biol.* **4**, 115 (2016).
24. Fink Jr, D. W. J. S. FDA regulation of stem cell-based products. *Science* **324**(5935), 1662–1663 (2009).
25. Hoang, V. T. et al. Standardized xeno- and serum-free culture platform enables large-scale expansion of high-quality mesenchymal stem/stromal cells from perinatal and adult tissue sources. *Cytotherapy* **23**(1), 88–99 (2021).
26. Almeria, C. et al. Hypoxia conditioned mesenchymal stem cell-derived extracellular vesicles induce increased vascular tube formation in vitro. *Front. Bioeng. Biotechnol.* **7**, 292 (2019).
27. Théry, C. et al. Minimal information for studies of extracellular vesicles 2018 (MISEV2018): a position statement of the International Society for Extracellular Vesicles and update of the MISEV2014 guidelines. *J. Extracell. Ves.* **7**(1), 1535750 (2018).
28. Hoang, D. H. et al. Differential wound healing capacity of mesenchymal stem cell-derived exosomes originated from bone marrow, adipose tissue and umbilical cord under serum- and xeno-free condition. *Front. Mol. Biosci.* **7**, 119 (2020).
29. Ahmadian, S. et al. Different storage and freezing protocols for extracellular vesicles: a systematic review. *Stem Cell Res. Ther.* **15**(1), 453 (2024).
30. Halme, D. G. FDA regulation of stem-cell-based therapies. *New England J. Med.* **355**(16), 1730 (2006).
31. Sun, L. et al. Safety evaluation of exosomes derived from human umbilical cord mesenchymal stromal cell. *Cytotherapy* **18**(3), 413–422 (2016).
32. Shulman, I. et al. Intrathecal injection of autologous mesenchymal stem-cell-derived extracellular vesicles in spinal cord injury: A feasibility study in pigs. *Int. J. Mol. Sci.* **24**(9), 8240 (2023).
33. Li, C. et al. Mesenchymal stromal cells ameliorate acute allergic rhinitis in rats. *Cell Biochem. Funct.* **35**(7), 420–425 (2017).
34. Gad, S. C. Rodent models for toxicity testing and biomarkers. In *Biomarkers in Toxicology* (ed. Gad, S. C.) (Elsevier, 2019).
35. Gupta, D. et al. Dosing extracellular vesicles. *Adv. Drug Deliv. Rev.* **178**, 113961 (2021).
36. Nair, A. B. A simple practice guide for dose conversion between animals and human. *J. Basic Clin. Pharm.* **7**(2), 27 (2016).
37. Rodrigues, S. C. et al. Toxicological profile of umbilical cord blood-derived small extracellular vesicles. *Membranes* **11**(9), 647 (2021).
38. Saleh, A. F. et al. Extracellular vesicles induce minimal hepatotoxicity and immunogenicity. *Nanoscale* **11**(14), 6990–7001 (2019).

## Author contributions

Quyen Thi Nguyen and Nhung Thi Dinh Hong: Conceptualization, Data curation, Formal analysis, Investigation, Methodology, Validation, Visualization, Writing original draft, Writing review & editing. Hang Ngo Thu, Can Van Mao, and Xuan-Hai Do: Investigation, Methodology, Validation, Visualization; Duc Son Le, Hong-Nhung Dao, and Ngan Giang T.: Data curation, Formal analysis, Investigation; Nicholas Forsyth: Writing, review & editing; Van T. Hoang and Liem Nguyen Thanh: Conceptualization, Data curation, Formal analysis, Investigation, Methodology, Supervision, Validation, Visualization, Writing – review & editing.

## Funding

This work is supported by the Vingroup Scientific Research Grant (Project number: PRO2178).

## Declarations

## Competing interests

The authors declare no competing interests.

## Ethics approval and consent to participate

Ethics approval for this project “Establishment of a serum-free and xeno-free culture of umbilical cord and adipose tissue derived mesenchymal stromal/stem cells in hypoxia condition, isolation, and characterization of extracellular vesicles, and evaluation of the safety and effectiveness of MSCs and exosomes for the treatment of spinal cord injury, lung fibrosis and dementia using animal models” was obtained from the Ethical Committee of Vinmec International Hospital (Approval No. 18/2022/CN-HĐĐĐ VMEC, dated 9th March 2022) and Dinh Tien Hoang Institute of Medicine, Vietnam (approval no. IRB-A-2201, dated 5th June 2022) in accordance with institutional guidelines and national ethical standards. Informed consent was obtained from volunteers prior to the collection of adipose tissue or umbilical cord samples.

## Consent for publication

All participants who voluntarily donated adipose tissue or umbilical cord provided written informed consent, agreeing to the use of their biological samples and associated data for research and publication purposes.

## Additional information

**Supplementary Information** The online version contains supplementary material available at <https://doi.org/10.1038/s41598-025-20121-7>.

**Correspondence** and requests for materials should be addressed to V.T.H. or L.N.T.

**Reprints and permissions information** is available at [www.nature.com/reprints](http://www.nature.com/reprints).

**Publisher's note** Springer Nature remains neutral with regard to jurisdictional claims in published maps and institutional affiliations.

**Open Access** This article is licensed under a Creative Commons Attribution-NonCommercial-NoDerivatives 4.0 International License, which permits any non-commercial use, sharing, distribution and reproduction in any medium or format, as long as you give appropriate credit to the original author(s) and the source, provide a link to the Creative Commons licence, and indicate if you modified the licensed material. You do not have permission under this licence to share adapted material derived from this article or parts of it. The images or other third party material in this article are included in the article's Creative Commons licence, unless indicated otherwise in a credit line to the material. If material is not included in the article's Creative Commons licence and your intended use is not permitted by statutory regulation or exceeds the permitted use, you will need to obtain permission directly from the copyright holder. To view a copy of this licence, visit <http://creativecommons.org/licenses/by-nc-nd/4.0/>.

© The Author(s) 2025